AIP | Applied Physics Letters

High-order harmonic generation at 4MHz as a light source for time-of-flight photoemission spectroscopy

Cheng-Tien Chiang, Alexander Blättermann, Michael Huth, Jürgen Kirschner, and Wolf Widdra

Citation: Appl. Phys. Lett. **101**, 071116 (2012); doi: 10.1063/1.4746264
View online: http://dx.doi.org/10.1063/1.4746264
View Table of Contents: http://apl.aip.org/resource/1/APPLAB/v101/i7
Published by the American Institute of Physics.

High-order harmonic generation at 4 MHz as a light source for time-of-flight photoemission spectroscopy

Cheng-Tien Chiang,[1,2] Alexander Blättermann,[2] Michael Huth,[1] Jürgen Kirschner,[1] and Wolf Widdra[1,2,a)]
[1]*Max Planck Institute of Microstructure Physics, Weinberg 2, D-06120 Halle, Germany*
[2]*Institute of Physics, Martin-Luther-Universität Halle-Wittenberg, Von-Danckelmann-Platz 3, D-06120 Halle(Saale), Germany*

(Received 8 June 2012; accepted 2 August 2012; published online 16 August 2012)

We demonstrate high-order harmonic generation (HHG) at 4 MHz driven by a long-cavity femtosecond laser oscillator. The laser output is used directly in a tight focusing geometry, where the harmonics are generated from a gas jet with high backing pressure. The harmonic light source is applied to time-of-flight photoemission spectroscopy, and the characteristic electronic structure of Cu(111) is measured. Our results suggest a straightforward design of high-order harmonic generation at megahertz repetition rate and pave the way for applications in electron spectroscopy and microscopy. © *2012 American Institute of Physics*. [http://dx.doi.org/10.1063/1.4746264]

The strong electric field in intense laser pulses can liberate bound electrons via tunnel ionization, accelerate free electrons in oscillatory pondermotive motion, and control electron-atom scattering for emission of high energy photons.[1] Coherent quantum mechanical combination of these three pathways leads to the high-order harmonic generation (HHG), whereby attosecond pulses of vacuum-ultraviolet and soft x-ray light can be produced in a laboratory setup.[2–5] Due to the ultrashort temporal duration and the widely tunable photon energy range of HHG-based light sources, their applications in electron microscopy and spectroscopy have great potential for studies of ultrafast electron dynamics in atomic, molecular, and condensed matter systems.[6–9]

Despite the long-term development of HHG since more than two decades, the design of HHG setups is still in rapid evolution.[10–12] Conventional HHG experiments are driven by amplified laser pulses at kilohertz frequency and can provide high photon energy up to several hundred electronvolts with moderate intensity. However, the statistics of experiments are limited by the rather low repetition rates, which result in a long acquisition time for applications in spectroscopy[13–16] and microscopy.[17,18] Especially, for photoelectron-based techniques, the overall counting rate is limited by the laser repetition rate due to energy and momentum broadening by space-charge effects.[19–22]

To increase the repetition rate of HHG, the driving laser with a typical average power of several watts needs to deliver more light pulses per unit time.[10] Consequently, the electric field strength decreases, and the HHG efficiency is dramatically reduced. Recently, three different approaches have been demonstrated in order to boost the repetition rate of HHG. Vernaleken *et al.*[23] and Hädrich *et al.*[24] used high power fiber-based lasers and amplifiers. They are able to generate the 17th harmonic at 20.8 MHz repetition rate using a sophisticated laser system with 20 W output power. Alternatively, to avoid using complex amplifier systems, Kim *et al.* used optically excited plasmons in microstructures to enhance the driving electric field.[25,26] Although they reported HHG up to 80 MHz, this approach and these results are currently under critical debate due to damages in the microstructures caused by the intense field.[27] The third approach is to generate harmonics inside the cavity of a resonator, either external to or implemented in the driving laser.[28,29] With additional efforts optimizing the output coupler for harmonics, Cingöz *et al.*[30] generated harmonics up to the 23rd order at 154 MHz and used their comb structure to characterize the line width of atomic transitions.

In this Letter, we report a more compact setup for HHG at megahertz repetition rate. We use directly the output of a Ti-sapphire laser at 4 MHz to generate harmonics up to 19th order from an Ar gas jet. With the generated light, we demonstrate a proof-of-principle application in the time-of-flight photoelectron spectroscopy. Our results provide a straightforward method for HHG at high repetition rate and pave the way to HHG-based electron microscopy and spectroscopy.

We use a long-cavity Ti-sapphire laser to drive the HHG.[31] The laser has a repetition rate of 4 MHz with a pulse width of 50 fs and an average power of 2.6 W centered around 800 nm. The long laser cavity is folded in restricted space by using a Herriott cell. After passing through a pair of prisms for control of pulse width, the laser beam is expanded to a diameter of about 15 mm and then focused by an achromatic lens into a gas jet in the generation chamber. The setup is shown in Fig. 1(a). The focal length of the lens is 50 mm and the laser focus has a diameter of 5 μm. The gas jet of Ar or Xe is produced by a glass capillary with a 30 μm circular opening.[32] With a 3 bar backing pressure of the gas jet, the pressure inside the generation chamber rises to 6×10^{-3} mbar, with a partial pressure of residual gas below 1×10^{-7} mbar.

After the harmonics are generated in the gas jet, they pass through a pin hole with a diameter of 200 μm, which separates the generation from the monochromator chamber. The monochromator chamber is differentially pumped and has a pressure below 2×10^{-7} mbar during HHG experiments. As shown schematically in Fig. 1(a), the generated high-order harmonics are diffracted by a toroidal grating in the monochromator chamber[33] and focused on the detector, which consists of two stacked channelplates and a phosphor

a)Electronic mail: wolf.widdra@physik.uni-halle.de.

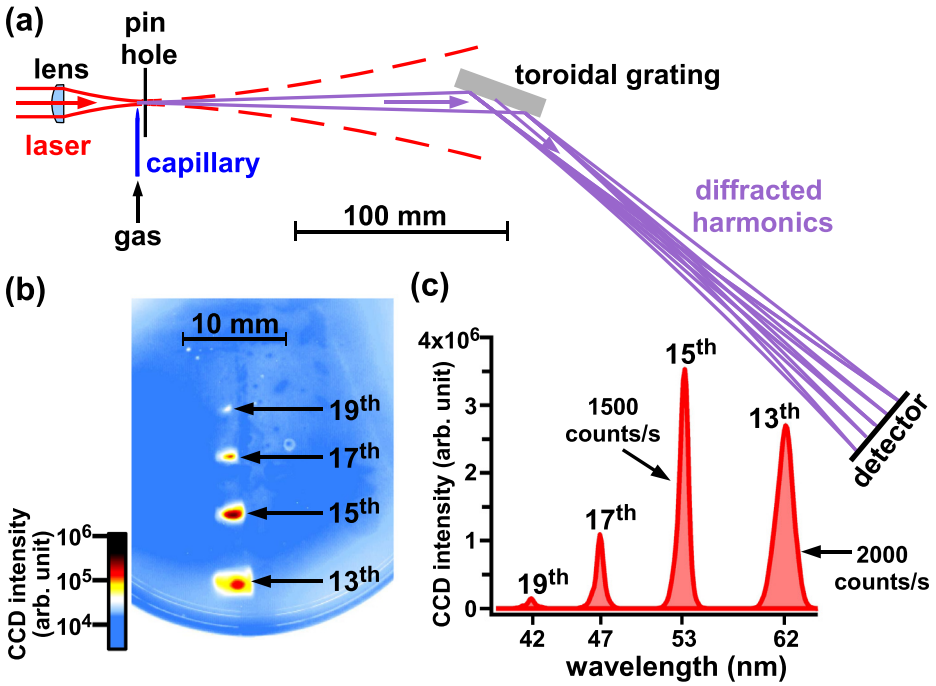

FIG. 1. (a) Geometry of the setup. Incident laser is linearly *s*-polarized with respect to the grating. (b) Image of the diffracted harmonics on the detector. The Ar gas jet has a backing pressure of 3.5 bar. (c) Line profile of the harmonics in (b) along the wavelength dispersive direction. The intensity of each harmonic is integrated laterally and the background is removed.

screen.[34] The fluorescence from the phosphor screen is measured by a CCD camera, which can be operated in an event-counting mode for calibration of the count rate of HHG photons. In Fig. 1(b), the image of the diffracted harmonics generated from Ar is shown. The HHG spectrum with estimated count rate is presented in Fig. 1(c).

The harmonics can be tuned by using different gases. In Fig. 2, we compare the HHG spectra from Xe and Ar. The spectra were measured with identical geometry and a backing pressure of 3 bar. The intensity of the 9th and 11th harmonics from Xe are about 800 and 10 times more intense than from Ar, respectively. In contrast to HHG from Ar, the harmonics from Xe are limited to the 11th order. The observed difference between HHG in Ar and in Xe is consistent with the known dependence of the ionization potential.[35] With the same driving electric field, the probability of tunnel ionization is higher in Xe due to its lower ionization potential as compared to Ar, explaining the higher HHG intensity from Xe. The lower cutoff energy in the HHG spectrum from Xe can as well be explained, since the energy of the electron before recombination and photon generation scales with the ionization potential.

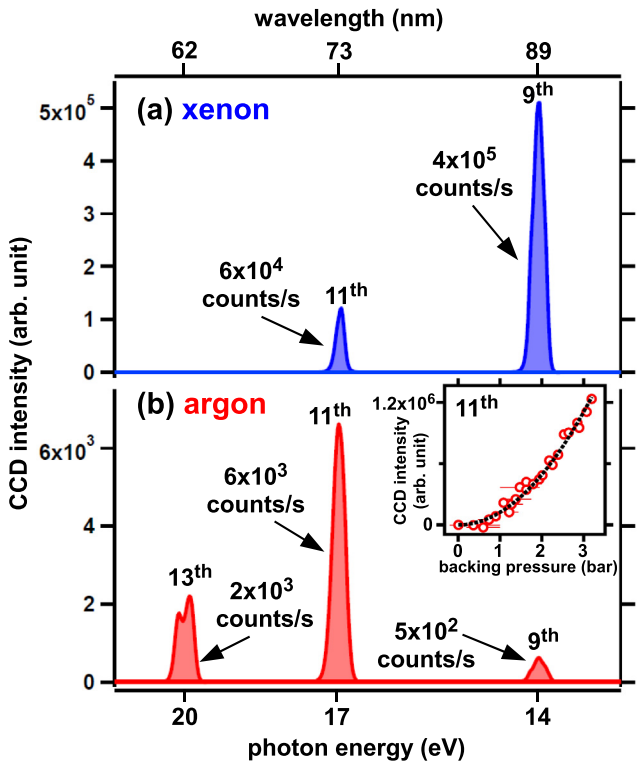

FIG. 2. Spectra of high-order harmonics generated within (a) Xe and (b) Ar jets. In both cases, the backing pressure of the gas jet is 3 bar. In the inset of (b), the backing pressure dependence of the 11th harmonic from the Ar jet is shown.

In addition to the features in the HHG spectra that can be interpreted qualitatively by the microscopic response of a single atom, the macroscopic generation of harmonic radiation relies on the coherent buildup of the electric field generated inside the laser-gas interaction volume.[5,12,36] Ideally, the HHG intensity reaches its maximum when the generated harmonics from all gas atoms in the laser focus can be constructively summed up. The constructive superposition requires a constant phase difference between the driving and the generated electric fields in space and time and is called phase-matching condition. In experiments, increasing the repetition rate while keeping the same intensity in the laser focus usually requires a tighter focusing. The tighter focusing geometry deteriorates the phase-matching condition due to a space-dependent Gouy phase.[37] In addition, the number of gas atoms in the interaction volume decreases rapidly as the focus size decreases. Heyl *et al.* have proposed to increase the gas jet pressure and to use the optical dispersion of gases to compensate for the Gouy phase.[11] Moreover, the number of gas atoms in the jet rises with increasing pressure. In our setup with tight focusing, we use a backing pressure up to several bars as shown in the inset of Fig. 2(b) for the 11th harmonic from the Ar jet. The intensity of the 11th

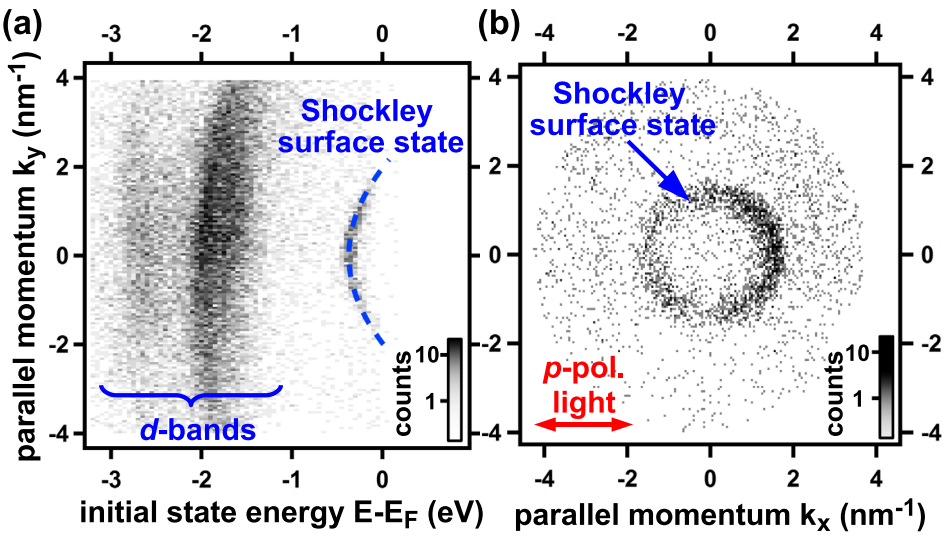

FIG. 3. (a) Photoemission spectra from Cu(111) along the $\overline{\Gamma K}$ direction. The dispersion of the Shockley surface state is observed (dashed curve).[40,41] (b) Momentum distribution of photoelectrons coming from 0.1 eV below the Fermi level. This measurement was done with the 9th harmonic in Xe with photon energy about 14 eV. The harmonic is linearly *p*-polarized with a projection onto the sample surface as indicated by the arrow.

harmonic increases quadratically with the backing pressure (dashed curve), implying a constant phase-matching condition up to 3 bar.[11] Note that our capillary with small opening makes it possible to operate at this pressure range with limited pumping speed. Additionally, the distribution of gas produced by the capillary is more local than in typical gas cells, minimizing the reabsorption of generated harmonics.[11] Since we did not observe a saturated nor a super quadratic backing pressure dependence of HHG, the backing pressure for optimal phase-matching condition is estimated to be above 3 bar.

We use the generated harmonics as an excitation source for time-of-flight photoemission spectroscopy. Therefore, the channelplate detector in Fig. 1(a) is replaced by a Cu(111) sample located in an ultrahigh vacuum chamber. Additionally, a pin hole with a diameter of 1.5 mm is used to filter the chosen harmonic and to separate the monochromator and the photoemission chambers. This results in an additional rare gas background pressure in the photoemission chamber below 2×10^{-9} mbar during the operation of HHG. The Cu(111) sample surface is cleaned by standard sputtering and annealing procedure and is checked by low-energy electron diffraction. Photoelectrons are collected by an electrostatic time-of-flight spectrometer,[38,39] which is mounted at 45° with respect to the incident HHG light. The sample is positioned in normal emission geometry. The time-of-flight of photoelectrons are referenced to the time at which HHG pulses excite the sample surface.

Figure 3 shows valence band photoemission data for a photon energy of 14 eV (9th harmonic from a Xe jet) with an acquisition time of 42 min. All photoelectrons with photoemission angles between ±15° were recorded simultaneously. From the three dimensional data set with respect to photoelectron energy and momenta parallel to the sample surface, two-dimensional cuts are shown in Figs. 3(a) and 3(b). In Fig. 3(a), in the energy range from 3 eV below the Fermi level (E_F) up to E_F, the distribution of photoelectrons having a wave vector within $\pm 4\,nm^{-1}$ parallel to $\overline{\Gamma K}$ in the surface Brillouin zone is shown. Near E_F, we observed the characteristic dispersion of the Shockley surface state on Cu(111) surface, which can be described by a parabolic dispersion with an effective mass of 0.4 times the electron mass and a binding energy of 0.37 eV (blue dashed curve).[40,41] At lower energies around 2 eV below E_F, we observed less dispersive features with higher photoemission intensity. These features are attributed to photoemission from copper *d*-bands with lower dispersion and a higher density of states. In Fig. 3(b), we show the momentum distribution of photoelectrons from 0.1 eV below E_F. The circular feature corresponds to photoemission from the Shockley surface state with two-dimensional free-electron-like dispersion.

To summarize, we demonstrate the HHG at 4 MHz repetition rate by directly using the output of a Ti-sapphire laser oscillator. The generation relies on a tight focusing of the laser light into a gas jet with high backing pressure. Moreover, we use the HHG light for time-of-flight photoemission spectroscopy and measure the characteristic electronic structure of the Cu(111) surface. Our results suggest a straightforward method to increase the repetition rate of HHG, providing a basis of efficient applications to photoelectron spectroscopies and microscopy.

The authors thank J. Güdde and C. Heyl for fruitful discussions. Support from R. Kulla, K. Duncker, M. Kiel, R. Neumann, and M. Schröder is gratefully acknowledged. M.H. would like to thank financial support by the DFG through SFB 762.

[1]P. B. Corkum, Phys. Today **64**, 36 (2011).
[2]M. Ferray, A. L'Huillier, X. F. Li, L. A. Lompre, G. Mainfray, and C. Manus, J. Phys. B **21**, L31 (1988).
[3]P. B. Corkum, Phys. Rev. Lett. **71**, 1994 (1993).
[4]F. Krausz and M. Ivanov, Rev. Mod. Phys. **81**, 163 (2009).
[5]T. Popmintchev, M.-C. Chen, P. Arpin, M. M. Murnane, and H. C. Kapteyn, Nature Photon. **4**, 822 (2010).
[6]M. Nisoli and G. Sansone, Prog. Quantum Electron. **33**, 17 (2009).
[7]J. Itatani, J. Levesque, D. Zeidler, H. Niikura, H. Pepin, J. C. Kieffer, P. B. Corkum, and D. M. Villeneuve, Nature (London) **432**, 867 (2004).
[8]A. L. Cavalieri, N. Müller, T. Uphues, V. S. Yakovlev, A. Baltuska, B. Horvath, B. Schmidt, L. Blumel, R. Holzwarth, S. Hendel, M. Drescher, U. Kleineberg, P. M. Echenique, R. Kienberger, F. Krausz, and U. Heinzmann, Nature (London) **449**, 1029 (2007).
[9]T. Haarlammert and H. Zacharias, Curr. Opin. Solid State Mater. Sci. **13**, 13 (2009).
[10]T. Südmeyer, S. V. Marchese, S. Hashimoto, C. R. E. Baer, G. Gingras, B. Witzel, and U. Keller, Nature Photon. **2**, 599 (2008).
[11]C. M. Heyl, J. Güdde, A. L'Huillier, and U. Höfer, J. Phys. B **45**, 074020 (2012).
[12]C. Winterfeldt, C. Spielmann, and G. Gerber, Rev. Mod. Phys. **80**, 117 (2008).

[13]P. Wernet, J. Gaudin, K. Godehusen, O. Schwarzkopf, and W. Eberhardt, Rev. Sci. Instrum. **82**, 063114 (2011).
[14]E. Magerl, S. Neppl, A. L. Cavalieri, E. M. Bothschafter, M. Stanislawski, T. Uphues, M. Hofstetter, U. Kleineberg, J. V. Barth, D. Menzel, F. Krausz, R. Ernstorfer, R. Kienberger, and P. Feulner, Rev. Sci. Instrum. **82**, 063104 (2011).
[15]G. L. Dakovski, Y. Li, T. Durakiewicz, and G. Rodriguez, Rev. Sci. Instrum. **81**, 073108 (2010).
[16]S. Mathias, L. Miaja-Avila, M. M. Murnane, H. Kapteyn, M. Aeschlimann, and M. Bauer, Rev. Sci. Instrum. **78**, 083105 (2007).
[17]S. H. Chew, F. Sussmann, C. Spath, A. Wirth, J. Schmidt, S. Zherebtsov, A. Guggenmos, A. Oelsner, N. Weber, J. Kapaldo, A. Gliserin, M. I. Stockman, M. F. Kling, and U. Kleineberg, Appl. Phys. Lett. **100**, 051904 (2012).
[18]A. Mikkelsen, J. Schwenke, T. Fordell, G. Luo, K. Klunder, E. Hilner, N. Anttu, A. A. Zakharov, E. Lundgren, J. Mauritsson, J. N. Andersen, H. Q. Xu, and A. L'Huillier, Rev. Sci. Instrum. **80**, 123703 (2009).
[19]J. Graf, S. Hellmann, C. Jozwiak, C. L. Smallwood, Z. Hussain, R. A. Kaindl, L. Kipp, K. Rossnagel, and A. Lanzara, J. Appl. Phys. **107**, 014912 (2010).
[20]S. Passlack, S. Mathias, O. Andreyev, D. Mittnacht, M. Aeschlimann, and M. Bauer, J. Appl. Phys. **100**, 024912 (2006).
[21]A. Locatelli, T. O. Menteş, M. Á. Niño, and E. Bauer, Ultramicroscopy **111**, 1447 (2011).
[22]X. Zhou, B. Wannberg, W. Yang, V. Brouet, Z. Sun, J. Douglas, D. Dessau, Z. Hussain, and Z.-X. Shen, J. Electron Spectrosc. Relat. Phenom. **142**, 27 (2005).
[23]A. Vernaleken, J. Weitenberg, T. Sartorius, P. Russbueldt, W. Schneider, S. L. Stebbings, M. F. Kling, P. Hommelhoff, H.-D. Hoffmann, R. Poprawe, F. Krausz, T. W. Hänsch, and T. Udem, Opt. Lett. **36**, 3428 (2011).
[24]S. Hädrich, M. Krebs, J. Rothhardt, H. Carstens, S. Demmler, J. Limpert, and A. Tünnermann, Opt. Express **19**, 19374 (2011).
[25]S. Kim, J. Jin, Y.-J. Kim, I.-Y. Park, Y. Kim, and S.-W. Kim, Nature (London) **453**, 757 (2008).
[26]I.-Y. Park, S. Kim, J. Choi, D.-H. Lee, Y.-J. Kim, M. F. Kling, M. I. Stockman, and S.-W. Kim, Nature Photon. **5**, 677 (2011).
[27]M. Sivis, M. Duwe, B. Abel, and C. Ropers, Nature (London) **485**, E1 (2012).
[28]C. Gohle, T. Udem, M. Herrmann, J. Rauschenberger, R. Holzwarth, H. A. Schuessler, F. Krausz, and T. W. Hänsch, Nature (London) **436**, 234 (2005).
[29]E. Seres, J. Seres, and C. Spielmann, Opt. Express **20**, 6185 (2012).
[30]A. Cingöz, D. C. Yost, T. K. Allison, A. Ruehl, M. E. Fermann, I. Hartl, and J. Ye, Nature (London) **482**, 68 (2012).
[31]Femtosource scientific XL 650, Femtolasers Produktions GmbH, Vienna, Austria.
[32]Micropipette made from borosilicate glass, Hilgenberg GmbH, Malsfeld, Germany.
[33]MBS M-1 VUV monochromator, 1200 lines/mm, MB Scientific AB, Uppsala, Sweden.
[34]BOS-40-6 beam observation system, Beam Imaging Solutions, Longmont, USA.
[35]M. Lewenstein, P. Balcou, M. Y. Ivanov, A. L'Huillier, and P. B. Corkum, Phys. Rev. A **49**, 2117 (1994).
[36]P. Balcou and A. L'Huillier, Phys. Rev. A **47**, 1447 (1993).
[37]F. Lindner, W. Stremme, M. G. Schätzel, F. Grasbon, G. G. Paulus, H. Walther, R. Hartmann, and L. Strüder, Phys. Rev. A **68**, 013814 (2003).
[38]Themis 1000, SPECS Surface Nano Analysis GmbH, Berlin, Germany.
[39]M. H. Berntsen, O. Gotberg, and O. Tjernberg, Rev. Sci. Instrum. **82**, 095113 (2011).
[40]A. A. Ünal, C. Tusche, S. Ouazi, S. Wedekind, C.-T. Chiang, A. Winkelmann, D. Sander, J. Henk, and J. Kirschner, Phys. Rev. B **84**, 073107 (2011).
[41]F. Reinert, G. Nicolay, S. Schmidt, D. Ehm, and S. Hüfner, Phys. Rev. B **63**, 115415 (2001).